

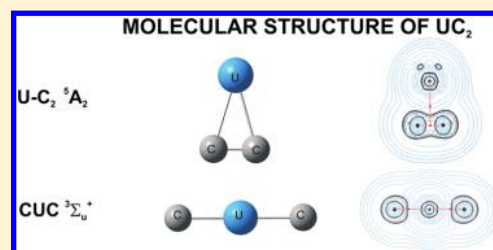
# On the Molecular Structure of Uranium Dicarbide: T-Shape versus Linear Isomers

M. Fernanda Zalazar,<sup>\*,†,‡,§</sup> Víctor M. Rayón,<sup>†</sup> and Antonio Largo<sup>†</sup>

<sup>†</sup>Departamento de Química Física y Química Inorgánica, Facultad de Ciencias, Universidad de Valladolid, 47005 Valladolid, Spain

<sup>‡</sup>Laboratorio de Estructura Molecular y Propiedades, Área de Química Física—Departamento de Química, Facultad de Ciencias Exactas y Naturales y Agrimensura, Universidad Nacional del Nordeste, Avenida Libertad 5460, (3400) Corrientes, Argentina

**ABSTRACT:** A theoretical study of the molecular structure of uranium dicarbide has been carried out employing DFT, coupled cluster, and multiconfigurational methods. A triangular species, corresponding to a  ${}^5A_2$  electronic state, has been found to be the most stable  $UC_2$  species. A triplet linear CUC species, which has been observed in recent infrared spectroscopy experiments, lies much higher in energy. A topological analysis of the electronic density has also been carried out. The triangular species is shown to be in fact a T-shape structure with a U–C interaction which can be considered to be a closed-shell interaction.



## INTRODUCTION

Solid uranium carbides have received much attention due to their role as appropriate fuels for new generations of nuclear reactors.<sup>1</sup> In particular, their thermodynamic properties and crystal structures have been investigated. On the other hand, little is known about uranium carbides in the gas phase, despite vaporization of uranium carbides occurring during their use as nuclear fuels. Some time ago high-temperature mass spectrometric studies<sup>2–4</sup> identified a variety of uranium carbides ranging from UC to UC<sub>6</sub>. Subsequent experimental work<sup>5</sup> on uranium carbides in the gas phase identified UC<sub>2</sub> and UC<sub>2</sub><sup>+</sup> as some of the most abundant molecular species.

In a very recent experimental study Wang et al.<sup>6</sup> produced uranium–carbon compounds through laser evaporation of uranium–carbon alloys followed by atom reaction in an argon matrix. The analysis of the infrared spectra of the reaction products, together with density functional theory (DFT) and ab initio calculations at the CASPT2 level, led to the characterization of UC and UC<sub>2</sub>. According to this combined experimental–theoretical study, UC has a quintet ground state, whereas a linear CUC structure ( ${}^3\Sigma_u^+$  electronic state) with uranium–carbon triple bonds was found for uranium dicarbide.<sup>6</sup> In a subsequent study, Wang et al.<sup>7</sup> reported a triangular structure for UC<sub>2</sub> to be lower in energy, despite the observation that in the experiments only the linear CUC structure was present. The reported linear structure for UC<sub>2</sub> prompted our attention, since our previous experience with second-row,<sup>8</sup> third-row,<sup>9</sup> and d-block<sup>10</sup> dicarbides has shown that electropositive elements tend to favor triangular ground-state structures. Given the low ionization energy of uranium (6.1941 eV) it should be expected to have a similar behavior.

In the present work we report the main results of our theoretical study of the molecular structure of uranium dicarbide, taking into account both linear and nonlinear structures as well as different spin multiplicities. We should

try to provide information that could be helpful in the interpretation of the experiments. An analysis of the bonding in the most relevant isomers of uranium dicarbide will also be carried out.

## COMPUTATIONAL METHODS

Different quantum chemistry methods have been employed. In the first place, molecular geometries have been obtained at the DFT level. In particular we used the B3LYP exchange–correlation functional.<sup>11,12</sup> In addition, geometrical optimizations have been performed at the CCSD (coupled-cluster single and double excitation model) level. Finally, CASPT2 (complete active space SCF corrected at the second-order perturbation theory) optimizations were also performed for the most relevant species. The active space in CASPT2 calculations was constructed including 10 electrons in 12 orbitals. In the case of the linear structure (see below) the active space comprises 6 bonding orbitals (two  $\sigma$  and two sets of  $\pi$  orbitals) and their corresponding antibonding orbitals correlating to the upper (occupied) and lower (unoccupied)  $\sigma$  and  $\pi$  components from the 5f, 6d, 7s, 7p (U), and 2p (O) atomic orbitals. For  $C_{2v}$ -symmetric structures the active space was chosen in an equivalent way: now, the active space comprises 6 orbitals from irrep  $a_1$ , 3 from  $b_1$ , 2 from  $b_2$ , and 1 from  $a_2$ . Different trials with larger active spaces showed no significant differences. Two different basis sets were employed: (i) a combination of the 6-311+G(3df) basis set<sup>13</sup> for carbon atom and the Stuttgart–Dresden effective core potential (ECP60MWB)<sup>14</sup> in conjunction with a [8s7p6d4f] basis set (referred to as “SDD” in Gaussian 03) for uranium; (ii) the all-electron ANO-RCC-VTZP basis set<sup>15</sup> (9s8p6d5f2g1h for uranium and of 4s3p2d1f

Received: October 26, 2011

Revised: January 18, 2012

Published: February 27, 2012

Table 1. Structural Properties for the Different UC<sub>2</sub> Species at Selected Levels of Theory

structure	method	geometry (Å, deg)			vibrational frequencies <sup>a</sup> (cm <sup>-1</sup> )	rotational constants (GHz)			
		d(UC)	d(CC)	∠CUC		A	B	C	μ (D)
CUC <sup>3</sup> Σ <sub>u</sub> <sup>+</sup>	B3LYP/6-311+G(3df)+SDD	1.834		180	976(σ <sub>w</sub> , 252), 918(σ <sub>g</sub> , 0), 110(π <sub>w</sub> , 88)		6.262		0.0
	CCSD/6-311+G(3df)+SDD	1.820		180	1005(σ <sub>w</sub> , 285), 965(σ <sub>g</sub> , 0), 56(π <sub>w</sub> , 128)		6.360		0.0
	CCSD/ANO-RCC-VTZP	1.829		180	987(σ <sub>w</sub> ), 933(σ <sub>g</sub> ), 120(π <sub>w</sub> )		6.288		0.0
	CASSCF(10,12)/ANO-RCC-VTZP	1.856		180	930(σ <sub>w</sub> , 100), 863(σ <sub>g</sub> , 0), 191(π <sub>w</sub> , 6)		6.107		0.0
	CASPT2(10,12)/ANO-RCC-VTZP	1.849		180					
U–C <sub>2</sub> <sup>5</sup> A <sub>2</sub>	B3LYP/6-311+G(3df)+SDD	2.291	1.261	32.0	1826(a <sub>1</sub> , 2), 508(a <sub>1</sub> , 130), 238(b <sub>2</sub> , 1)	52.977	4.779	4.384	6.598
	CCSD/6-311+G(3df)+SDD	2.284	1.266	32.2	1859(a <sub>1</sub> , 3), 519(a <sub>1</sub> , 173), 219(b <sub>2</sub> , 0)	52.554	4.814	4.410	6.634
	CCSD/ANO-RCC-VTZP	2.287	1.258	31.9		53.187	4.792	4.396	6.898
	CASSCF(10,12)/ANO-RCC-VTZP	2.332	1.250	31.1		53.898	4.589	4.229	7.410
	CASPT2(10,12)/ANO-RCC-VTZP	2.254	1.273	32.8		51.897	4.954	4.522	6.507
CUC <sup>1</sup> A <sub>1</sub>	B3LYP/6-311+G(3df)+SDD	1.818		134.1	941(a <sub>1</sub> , 3), 875(b <sub>2</sub> , 8), 169(a <sub>1</sub> , 36)	46.164	7.513	6.462	5.095
	CCSD/6-311+G(3df)+SDD	1.806		153.1	984(a <sub>1</sub> , 0), 869(b <sub>2</sub> , 88), 169(a <sub>1</sub> , 92)	131.18	6.824	6.486	3.309
U–C <sub>2</sub> <sup>3</sup> A <sub>2</sub>	B3LYP/6-311+G(3df)+SDD	2.289	1.261	32.0	1827(a <sub>1</sub> , 2), 504(a <sub>1</sub> , 128), 258(b <sub>2</sub> , 2)	52.992	4.789	4.392	6.291
	CCSD/6-311+G(3df)+SDD	2.279	1.266	32.2	1828(a <sub>1</sub> , 3), 510(a <sub>1</sub> , 177), 305(b <sub>2</sub> , 7)	52.552	4.834	4.427	6.694
CCU <sup>5</sup> Σ	B3LYP/6-311+G(3df)+SDD	2.133	1.272	180	1864(σ), 489(σ), 131 i(π)		2.857		9.717
	CCSD/6-311+G(3df)+SDD	2.125	1.275	180	1883(σ), 502(σ), 144 i(π)		2.868		9.844

<sup>a</sup>Mode symmetry and IR intensity (km/mol) in parentheses.

Table 2. Relative Energies (kcal/mol) at Selected Levels of Theory for the Most Relevant UC<sub>2</sub> Species<sup>a</sup>

	CUC <sup>3</sup> Σ <sub>u</sub> <sup>+</sup>	U–C <sub>2</sub> <sup>5</sup> A <sub>2</sub>	U–C <sub>2</sub> <sup>3</sup> A <sub>2</sub>	CUC <sup>1</sup> A <sub>1</sub>	CCU <sup>5</sup> Σ
B3LYP/6-311+G(d)+SDD	83.94	0.0	4.86	95.38	13.99
CCSD/6-311+G(d)+SDD	56.48 (65.14) <sup>b</sup>	0.0	5.21	66.04	17.32
CCSD(T)/6-311+G(d)+SDD	45.95 (56.61) <sup>b</sup>	0.0	4.23	48.22	17.93
CCSD/ANO-RCC-VTZP	73.25 <sup>b</sup>	0.0			
CCSD(T)/ANO-RCC-VTZP	64.12 <sup>b</sup>	0.0			
CASPT2(10,12)/ANO-RCC-VTZP	57.42	0.0			

<sup>a</sup>ZPE corrections have been included. <sup>b</sup>Relative energies computed with the ROHF-reference wave function as implemented in MOLPRO.

for carbon). Static relativistic effects are included in the Stuttgart–Dresden pseudopotential. For the all-electron basis set relativistic effects have been included through the use of a Douglas–Kroll–Hess Hamiltonian. Harmonic vibrational calculations have been performed at selected levels of theory in order to assess the nature of the stationary points on the potential energy surface as well as to estimate the zero-point energy (ZPE). The electronic energy has been refined by means of single-point calculations at the CCSD(T) level (CCSD augmented with a noniterative treatment of triple excitations).<sup>16</sup> All these calculations were carried out with the Gaussian 03<sup>17</sup> and MOLPRO<sup>18</sup> program packages.

The nature of the bonding in isomers of uranium dicarbide was characterized through the topological analysis of the electron charge density distribution,  $\rho(r)$ , in the framework of the atoms in molecules theory (AIM).<sup>19</sup> Total electron densities were obtained at B3LYP level with the 6-311+G(3df) basis set for carbon atom and the Stuttgart–Dresden effective core potential (SDD) for uranium. The bond properties were calculated using the AIM2000 package.<sup>20</sup>

## RESULTS AND DISCUSSION

We have searched for possible isomers of the UC<sub>2</sub> system, considering different spin multiplicities. Only the most significant species found in this search will be discussed in the present work. A summary of the main structural properties found for these species is given in Table 1. Their relative energies are collected in Table 2.

We have found a linear CUC isomer, with the same electronic state as predicted by Wang et al.,<sup>6</sup> that is, <sup>3</sup>Σ<sub>u</sub><sup>+</sup> [...

(π<sub>g</sub>)<sup>2</sup>(σ<sub>g</sub>)<sup>1</sup>(σ<sub>u</sub>)<sup>1</sup>(π<sub>u</sub>)<sup>2</sup>]. This is the species that has been observed in the experiments through its infrared spectrum. All theoretical methods give rise to a U–C bond distance that is relatively short, around 1.820–1.856 Å, and is also coincident in the relative IR intensities, with the antisymmetric stretching being the most intense signal in the IR spectrum. All theoretical methods predict a higher frequency for the antisymmetric stretching mode than that observed in the experiments in argon matrices,<sup>6</sup> namely 891.4 cm<sup>-1</sup>. This difference should be partially due to the argon matrix host used for the experiments since argon interacts more strongly with the guest molecules than lighter noble gases. Thus, we would expect a closer agreement of the theoretical predictions with a neon matrix value, as it was observed for UC, but unfortunately, CUC could not be detected in neon matrices. In addition, we should recall that the theoretical values provided in Table 1 are unscaled frequencies.

The lowest-lying singlet and quintet states for the CUC isomer have imaginary frequencies, and therefore cannot be considered true minima on their respective potential energy surfaces. In the case of the singlet we were able to characterize a bent minimum, <sup>1</sup>A<sub>1</sub> electronic state, whose structural parameters are shown in Table 1. The ∠CUC bond angle takes a value of 134.1° at the B3LYP level, whereas at the CCSD level it is around 153.1°. In any case, the geometry at both levels deviates considerably from linearity, as reflected in the rotational constants. The predicted dipole moment differs at both levels, as a consequence basically of the different bond angle, but in both cases takes a relatively high value.

**Table 3. Local Topological Properties (au) of the Electronic Charge Density Distribution Calculated at the Position of the Bond Critical Points for the Different UC<sub>2</sub> Species<sup>a</sup>**

species	bond	$\rho(r)$	$\nabla^2\rho(r)$	$\epsilon$	$ \lambda_1 /\lambda_3$	$ V(r) /G(r)$	$H(r)$
UC <sup>5</sup> X	U–C	0.2185	0.1336	0.0090	0.3725	1.8498	–0.1890
CUC <sup>3</sup> $\Sigma_u^+$	U–C	0.2319	0.1289	0.0000	0.3733	1.8671	–0.2102
CUC <sup>1</sup> A <sub>1</sub>	U–C	0.2565	–0.0956	0.4487	0.7027	2.1060	–0.2493
CCU <sup>5</sup> $\Sigma$	U–C	0.1469	0.1106	0.0018	0.3790	1.7438	–0.0803
	C–C	0.4015	–1.4055	0.0000	3.1640	3.8319	–0.5432
U–C <sub>2</sub> <sup>5</sup> A <sub>2</sub>	U–C	0.1035	0.2135	8.7897	0.3374	1.4087	–0.0369
	C–C	0.4010	–1.2888	0.1059	3.1981	3.4367	–0.5465
U–C <sub>2</sub> <sup>3</sup> A <sub>2</sub>	U–C	0.1041	0.2126	8.4469	0.3395	1.4125	–0.0373
	C–C	0.4004	–1.2836	0.1079	3.2022	3.4274	–0.5457

<sup>a</sup>The electronic charge density [ $\rho(r)$ ], the Laplacian [ $\nabla^2\rho(r)$ ], the ellipticity ( $\epsilon$ ), the relationship between the perpendicular and parallel curvatures ( $|\lambda_1|/\lambda_3$ ). The relationship between the local kinetic energy density [ $G(r)$ ] and the local potential energy density, [ $V(r)$ ], and the total energy density, [ $H(r)$ ].

We also considered possible structures where the uranium atom is located at a terminal position, giving rise to the CCU connectivity. In this case the lowest-lying states of the different multiplicities (singlet, triplet, and quintet) that were found are in fact transition states for the degenerate rearrangement of C<sub>2v</sub>-symmetric species, since all of them have imaginary  $\pi$  vibrational frequencies. The most stable linear CCU species corresponds to a <sup>5</sup> $\Sigma$  state, and this is the only species that will be briefly discussed. The U–C distance is considerably longer than that found for linear CUC, being much closer to those found for triangular species.

Finally, we have explored different electronic states for the triangular (C<sub>2v</sub>-symmetric) U–C<sub>2</sub> isomer. Several electronic states are close in energy, as a consequence of the different close-lying orbitals of the uranium atom. We will only report our results for the lowest-lying triplet and quintet states. The most stable triplet state corresponds to a <sup>3</sup>A<sub>2</sub> electronic state, resulting from a a<sub>1</sub><sup>2</sup>a<sub>1</sub><sup>2</sup>b<sub>1</sub><sup>1</sup>b<sub>2</sub><sup>1</sup> electronic configuration. On the other hand, the lowest-lying quintet state, <sup>5</sup>A<sub>2</sub>, results from an a<sub>1</sub><sup>2</sup>b<sub>2</sub><sup>1</sup>a<sub>1</sub><sup>1</sup>b<sub>1</sub><sup>1</sup>a<sub>1</sub><sup>1</sup> electronic configuration. It is interesting to point out that the <sup>5</sup>A<sub>2</sub> electronic state reported by Wang et al. in their last paper<sup>7</sup> as the most stable UC<sub>2</sub> species corresponds to a different electronic configuration (namely, a<sub>1</sub><sup>2</sup>b<sub>2</sub><sup>1</sup>a<sub>1</sub><sup>1</sup>b<sub>2</sub><sup>1</sup>a<sub>2</sub><sup>1</sup>). According to our calculations the <sup>5</sup>A<sub>2</sub> electronic state predicted in the present work is more stable than the previously reported by 6.2 kcal/mol (B3LYP level) or 5.1 kcal/mol (CCSD(T) level). In fact, there are even other quintet states (<sup>5</sup>A<sub>1</sub> and <sup>5</sup>B<sub>1</sub>) that are more stable than the <sup>5</sup>A<sub>2</sub> electronic state previously reported by Wang et al.<sup>7</sup> Our computed bond distances for the <sup>5</sup>A<sub>2</sub> and <sup>3</sup>A<sub>2</sub> states are very similar. The C–C bond distances in both cases suggest a strong C–C bonding, almost approaching a triple bond, whereas the U–C bond distance is relatively long, about 0.4 Å longer than the U–C distance found for the linear <sup>3</sup> $\Sigma_u^+$  species. The <sup>5</sup>A<sub>2</sub> and <sup>3</sup>A<sub>2</sub> states have also quite similar vibrational frequencies and IR intensities. Clearly in both cases the most intense line in the IR spectrum is predicted to be the U–C<sub>2</sub> stretching, with a frequency near 500 cm<sup>–1</sup>.

The relative energies at different levels of theory of the most relevant UC<sub>2</sub> species are given in Table 2. The most important result is that the <sup>5</sup>A<sub>2</sub> electronic state of the U–C<sub>2</sub> triangular isomer is predicted to be the lowest-lying state at all levels of theory. There is no doubt that this isomer should be the most stable one, since only the triplet state (<sup>3</sup>A<sub>2</sub>) of the same isomer is relatively close in energy. The difference between the <sup>5</sup>A<sub>2</sub> and <sup>3</sup>A<sub>2</sub> states of the triangular isomer is small, but is consistent at all levels of theory (between 4 and 5 kcal/mol). The CCU

species in its quintet state, which is predicted to be in fact a transition state as we have pointed out before, lies nearly 14 kcal/mol higher in energy than the <sup>5</sup>A<sub>2</sub> state at the B3LYP level, and this energy difference is even slightly increased at the CCSD(T) level up to nearly 18 kcal/mol. The linear CUC species, which has been observed in the experiments, is predicted to lie much higher in energy than the triangular <sup>5</sup>A<sub>2</sub> species. The energy difference in this case is rather sensible to the level of calculation employed. The B3LYP level predicts an energy difference of 83.94 kcal/mol. As in other systems with multiple bonding, a more rigorous account of correlation effects is important. Therefore, the energy difference with the triangular isomer is substantially reduced at the CCSD level, and especially when triple substitutions are taken into account. The CASPT2 results show also the same trend, leading to an energy difference between the linear and triangular isomers of 57.42 kcal/mol. Consideration of spin–orbit effects does not sensibly alter these conclusions about the relative stability of uranium dicarbide species. Our estimates of spin–orbit effects only modify the energy difference between the <sup>5</sup>A<sub>2</sub> species and the linear CUC isomer (two of the most different species) by nearly 3 kcal/mol. We have additionally searched for a transition state for the CUC (<sup>3</sup> $\Sigma_u^+$ ) → UC<sub>2</sub> rearrangement in the triplet surface in order to estimate the energy barrier that the linear isomer should surmount in order to give a cyclic structure. At the B3LYP/6-311+G(3df) the barrier is 18.2 kcal/mol (Wang et al. estimated 30 kcal/mol using a PBE functional<sup>7</sup>). This suggests that, once formed, CUC (<sup>3</sup> $\Sigma_u^+$ ) should be stable under the experimental conditions.<sup>7</sup> Finally, the bent CUC isomer (<sup>1</sup>A<sub>1</sub> electronic state) is predicted at all levels of theory to be even less stable than the linear CUC species.

The overall picture that can be extracted from the results shown in Table 2 is that those species with C–C bonding (triangular U–C<sub>2</sub> and linear CCU) are preferred over those species with the uranium atom inserted into a pair of carbon atoms (linear and bent CUC), despite the possibility of two multiple U–C bonds being formed in the latter case. This result is in contrast with the evidence that the linear CUC isomer, in its triplet ground state, is observed in the experiments. The most plausible explanation seems to be that provided by Wang et al.<sup>7</sup> These authors suggest that probably the amount of C<sub>2</sub> present in the matrix isolation experiments is too small to produce significant amounts of the triangular U–C<sub>2</sub> isomer, and therefore, the chemistry in the matrix experiments could be dominated by C atom reactions. Moreover, and as stated above,

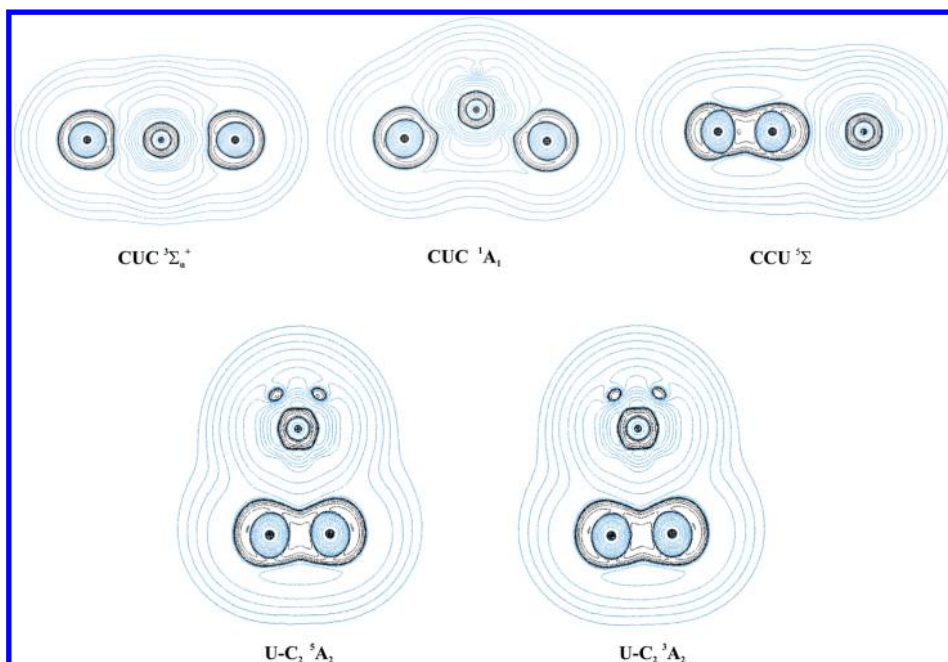


**Figure 1.** Contour maps of the Laplacian distribution of the electronic charge density for the different  $UC_2$  species. Black lines indicate regions of electronic charge concentration, and blue lines denote regions of electronic charge depletion.

once the linear CUC molecule is formed, its conversion into the most stable cyclic  $UC_2$  isomer should be hindered by a relatively large energy barrier. We would nevertheless like to point out that other possible explanations, such as possible secondary species formed from  $U-C_2(^5A_2)$ , should not be ruled out. For example, this species could form dimers,  $U_2C_4$  compounds, making undetectable the  $U-C_2$  triangular isomer. Some of these possibilities are currently explored in our group. Let us finally point out that in the solid phase,  $U-C_2$  presents a tetragonal phase with linear  $-U-CC-U-$  units with  $U-CC$  distances that are only a little shorter than the  $U-C$  distances from the perpendicular U centers occupying the adjacent interstices (2.321 vs 2.576 Å).<sup>21–24</sup>

The computed bond dissociation energy of  $C_{2v}$ -symmetric  $U-C_2$  isomer is 154.96 kcal/mol at the CCSD(T) level of theory in good agreement with a reported high temperature mass spectroscopic value of  $159 \pm 1$  kcal/mol.<sup>4</sup> This agreement suggests that the isomer formed in these gas-phase experiments corresponds to the  $C_{2v}$ -symmetric  $U-C_2$  species.

In order to characterize the nature of the bonding in the uranium dicarbide species, we have applied the topological analysis of the electronic charge density.<sup>19</sup> Within this formalism, critical points in the one-electron density,  $\rho(r)$ , are identified. In our case, uranium dicarbides, only bond critical points [corresponding to a minimum value of  $\rho(r)$  along the line connecting the nuclei and a maximum along the interatomic surfaces] and eventually ring critical points [ $\rho(r)$  being a minimum in two directions and a maximum in one direction] are relevant. A summary of the most relevant topological properties of the critical points is provided in Table 3.

In the case of linear or bent CUC and linear CCU species only C–U or C–C bond critical points (BCPs) can obviously be found. However, in the case of triangular  $U-C_2$  species it is interesting to identify possible ring critical points, in order to ascertain whether these isomers are true rings. As can be seen in Table 3, neither triplet nor quintet states of  $C_{2v}$ -symmetric  $U-$

$C_2$  exhibit a ring critical point. In these cases, in addition to the C–C bond critical point, only a bond critical point between the uranium atom and the middle point of the  $C_2$  unit can be found. Therefore, these species should be classified as T-shape structures rather than truly cyclic molecules, since no individual U–C bonds are characterized. This is not an unexpected behavior, since most first-row transition metals also give rise to T-shape dicarbides.<sup>10</sup>

The properties collected in Table 3 allow an analysis of the nature of the interaction between the uranium and carbon atoms in uranium dicarbide species. In addition some representative pictures of the contour maps of the Laplacian distributions of the electronic charge densities are provided in Figure 1. In Table 3 we have also included for comparison purposes the topological analysis of the charge density for the ground state of uranium monocarbide, UC.

We should briefly recall that the chemical nature of the bonding can be analyzed through the values of the electronic charge density and its Laplacian at the bond critical points. Two limiting types of interactions can be identified: shared interactions and closed-shell interactions.<sup>25</sup> Shared interactions are characterized essentially by large electron densities and negative values of the Laplacian, and are typical of covalent compounds. On the other hand, closed-shell interactions correspond to relatively low values of  $\rho(r)$  and positive values of its Laplacian, and are characteristic of ionic and van der Waals compounds. Nevertheless, we should point out that there is a whole spectrum of intermediate interactions lying between these two limiting cases.<sup>25</sup> There is another particularly interesting property, the total energy density  $H(r)$  (defined as the sum of the potential and kinetic energy densities at a critical point) which is also useful to characterize the degree of covalency of a bond. If  $H(r)$  is negative, the system is stabilized by the accumulation of electronic charge in the internuclear region, which is a typical characteristic of a covalent interaction.<sup>26</sup> On the other hand, when  $H(r)$  is positive accumulation of charge density in the region between

the nuclei leads to a destabilization of the system, which is the behavior observed for ionic interactions and van der Waals systems.<sup>26</sup>

From the results collected in Table 3 and the contour maps represented in Figure 1 we can see that the U–C interactions can be classified as closed-shell interactions. This is particularly evident in Figure 1 when comparing U–C interactions with the C–C interaction in the T-shape isomer. Whereas in the C–C bond the two valence shell concentrations merge with each other to give a single region of bonding charge concentration (shared interaction), all U–C interactions give typical contours of closed-shell interactions.

In the linear CUC isomer the U–C bonds show properties virtually identical to those found for the monocarbide, UC. In both cases, UC and CUC, the U–C bonds show a moderate value of  $\rho(r)$  and a positive value for  $\nabla^2\rho(r)$  (local depletion of charge density). These properties are clearly indicative of a closed-shell interaction. The ellipticity takes a value of zero and the  $|\lambda_1/\lambda_3|$  is appreciably lower than 1. In addition, the total energy density,  $H(r)$ , shows a negative value which suggests some degree of covalency. Besides, the covalent character of an interaction can also be quantitatively analyzed by taking into account the  $|V(r)|/G(r)$  relationship. This relationship shows values greater than 2 for covalent interactions, smaller than 1 for noncovalent interactions, and between 1 and 2 for partially covalent bonds. In other words, the  $|V(r)|/G(r)$  ratio may be treated as a measure of the “covalence” of a bonding interaction. The value shown in Table 3 ( $|V(r)|/G(r) = 1.86$ ) indicates that the U–C bonds in the linear CUC isomer can be described as closed shell interactions with a partially covalent character.

In the bent CUC isomer ( ${}^1A_1$  electronic state) it can be observed that the electronic charge density at the U–C bond critical point increases, and the Laplacian of  $\rho(r)$  is slightly negative,  $|V(r)|/G(r) > 2$ , and  $G(r)/\rho(r) < 1$ . All these characteristics indicate that this species, although maintaining the basic characteristics of a closed-shell interaction, approaches somewhat the features of shared interactions.

The T-shape structures, corresponding to  ${}^3A_2$  and  ${}^5A_2$  states, exhibit very similar characteristics. The U–C bond critical point shows a relatively low density value (smaller than in the linear isomer, but greater than 0.1 au), positive values of the Laplacian, and  $|\lambda_1/\lambda_3| < 1$ , all of them characteristic of closed-shell interactions. However, a small but negative value of the total energy density suggests a small degree of covalence. All the results collected in Table 3 suggest that U–C<sub>2</sub> interactions in the T-shape species are less covalent (or greater ionic character) than in the linear CUC isomer in terms of their smaller values of  $\rho(r)$ ,  $|V(r)|/G(r)$ , and  $H(r)$ , and greater positive values of  $\nabla^2\rho(r)$ .

In the CCU species ( ${}^5\Sigma$  electronic state), the U–C bond critical point shows a low value of  $\rho(r)$  and a positive value for  $\nabla^2\rho(r)$ ,  $\epsilon$  value is near to zero, and  $H(r)$  is negative. The  $|V(r)|/G(r)$  values of the U–C bond are lower than the U–C bond in CUC isomer and higher than the U–C bond in U–C<sub>2</sub>; consequently, the covalent character in this species seems to be intermediate between the linear and the T-shape isomers.

Therefore, it seems that from a global perspective the U–C interactions in the different uranium dicarbide structures can be described as intermediate interactions, but basically they correspond to predominantly ionic interactions with some degree of covalence. In particular, for the most stable structure, the T-shape U–C<sub>2</sub> isomer, the U–C interaction shows a very

small covalent character and the interaction is much more ionic. The ionic nature of the U–C interactions is also reflected in the relatively high dipole moments obtained for the different UC<sub>2</sub> species (except for the linear CUC isomer, obviously for reasons of symmetry). Finally, we have calculated the atomic charges obtained by integrating the charge density over the atomic basin. The accuracy of the integration was assessed by the magnitude of a function  $L(\Omega)$ , which in all cases is minor to  $10^{-4}$  au. The net atomic charge,  $q(\Omega)$ , on the uranium atom shows a value of +1.18 au in the U–C<sub>2</sub>  ${}^5A_2$  in agreement with the partial ionic character of the bonding. Interestingly, in spite of the larger covalent character of the U–C bonds, we found a larger net charge for uranium in linear CUC  ${}^3\Sigma_u^+$ , namely, +1.72 au. Thus, and in agreement with the previous discussion, bonding in CUC should be highly polar for this electronic state. Let us also briefly address the spin density distribution on the  ${}^5A_2$  and  ${}^3\Sigma_u^+$  states. For the former, the integrated spin density yields 3.94 electrons in U whereas for the linear isomer we find a more even distribution: U, 1.01 electron. For the cyclic isomer, this spin density distribution is compatible with a formal U<sup>2+</sup>–C<sub>2</sub><sup>2-</sup> donor–acceptor interaction in which the dicarbide anion donates about 1 electron to the uranium fragment (let us also point out that the four singly occupied molecular orbitals in this state are, in essence, 5f atomic orbitals). For the linear CUC molecule, the spin density can be easily explained in terms of its electronic configuration with two singly occupied  $\sigma$  orbitals showing a similar weighting of the U and C atomic orbitals.

## CONCLUSIONS

A theoretical study of the molecular structure of uranium dicarbide has been carried out. We have considered both linear and nonlinear structures, as well as different spin multiplicities. All levels of theory employed in the present work (DFT, CC, CASPT2) agree in that the most stable species should be a triangular ( $C_{2v}$ -symmetric) isomer with a  ${}^5A_2$  electronic state. It is interesting pointing out that the  ${}^5A_2$  state reported in the present work corresponds to a different electronic configuration as the one reported in a previous work.<sup>7</sup> In agreement with previous studies by other authors,<sup>6,7</sup> the linear CUC isomer identified through infrared spectroscopy experiments should be considerably less stable (around 57 kcal/mol higher in energy than the triangular species at the more reliable levels of theory).

A topological analysis of the electronic charge density has shown that in fact the  $C_{2v}$ -symmetric isomer is a T-shape species, since it shows no individual U–C bond critical points. The bond critical point is found along the line connecting the uranium atom and the middle point of the C–C bond. In addition, the U–C interaction shows characteristics of typical closed-shell interactions, suggesting a predominantly ionic U–C<sub>2</sub> bonding. The linear CUC species also shows typical features of closed-shell interactions, but in this case the U–C interaction has some degree of covalent character.

## AUTHOR INFORMATION

### Corresponding Author

\*E-mail: mfmzalar@conicet.gov.ar. Fax: +54-379-4473930.

### Notes

The authors declare no competing financial interest.

<sup>§</sup>On leave from Universidad Nacional del Nordeste.

## ACKNOWLEDGMENTS

This research has been supported by the Ministerio de Ciencia e Innovación of Spain (Grant CTQ2010-16864) and by the Junta de Castilla y León (Grant VA040A09). M.F.Z. gratefully acknowledges a grant from the Eurotango Erasmus Mundus Program that made possible her stay at Valladolid. M.F.Z. also acknowledges the Universidad Nacional del Nordeste and Consejo Nacional de Investigaciones Científicas y Técnicas of Argentina (CONICET).

## REFERENCES

- (1) Utton, C. A.; De Bruycker, F.; Boboridis, K.; Jardin, R.; Noel, H.; Gueneau, C.; Manara, D. *J. Nucl. Mater.* **2009**, *385*, 443.
- (2) Norman, J. H.; Winchell, P. *J. Phys. Chem.* **1964**, *68*, 3802.
- (3) Gingerich, K. A. *J. Chem. Phys.* **1969**, *50*, 2255.
- (4) Gupta, S. K.; Gingerich, K. A. *J. Chem. Phys.* **1979**, *71*, 3072.
- (5) Datta, B. P.; Sant, V. L.; Raman, V. A.; Subbanna, C. S.; Jain, H. *C. Int. J. Mass Spectrom. Ion Processes* **1989**, *91*, 241.
- (6) Wang, X.; Andrews, L.; Malmqvist, P. A.; Roos, B. O.; Gonçalves, A. P.; Pereira, C. C. L.; Marçalo, J.; Godart, C.; Villeroy, B. *J. Am. Chem. Soc.* **2010**, *132*, 8484.
- (7) Wang, X.; Andrews, L.; Ma, D.; Gagliardi, L.; Gonçalves, A. P.; Pereira, C. C. L.; Marçalo, J.; Godart, C.; Villeroy, B. *J. Chem. Phys.* **2011**, *134*, 244313.
- (8) Largo, A.; Redondo, P.; Barrientos, C. *J. Am. Chem. Soc.* **2004**, *126*, 14611.
- (9) Rayon, V. M.; Redondo, P.; Barrientos, C.; Largo, A. *J. Chem. Phys.* **2010**, *133*, 124306.
- (10) Rayon, V. M.; Redondo, P.; Barrientos, C.; Largo, A. *Chem.—Eur. J.* **2006**, *12*, 6963.
- (11) Becke, A. D. *J. Chem. Phys.* **1986**, *84*, 4524.
- (12) Becke, A. D. *J. Chem. Phys.* **1988**, *88*, 2547.
- (13) Krishnan, R.; Binkley, J. S.; Seeger, R.; Pople, J. A. *J. Chem. Phys.* **1980**, *72*, 650.
- (14) Kuechle, W.; Dolg, M.; Stoll, H.; Preuss, H. *J. Chem. Phys.* **1994**, *100*, 7535.
- (15) Roos, B. O.; Lindh, R.; Malmqvist, P. A.; Veryazov, V.; Widmark, P. O. *Chem. Phys. Lett.* **2005**, *409*, 295.
- (16) Raghavachari, K.; Trucks, G. W.; Pople, J. A.; Head-Gordon, M. *Chem. Phys. Lett.* **1989**, *157*, 479.
- (17) Frisch, M. J.; et al. *Gaussian 03*; Gaussian Inc.: Pittsburgh, PA, 2003.
- (18) Werner H. J.; Knowles, P. J. *MOLPRO version 2002.1*; 2002.
- (19) Bader, R. W. F. *Atoms in Molecules: A Quantum Theory*; Clarendon Press, Oxford, U.K., 1990.
- (20) Blieger-König, F.; Schönbohn, J. *AIM 2000 Program Package, version 2.0*; Büro für Innovative Software Streibel Biegler-König: Bielefeld, Germany, 2002.
- (21) Atoji, M.; Medrud, R. C. *J. Chem. Phys.* **1959**, *31*, 332.
- (22) Atoji, M. *J. Chem. Phys.* **1961**, *35*, 1950.
- (23) Bowman, A. L.; Arnold, G. P.; Witteman, W. G.; Wallace, T. C.; Nereson, N. G. *Acta Crystallogr.* **1966**, *21*, 670.
- (24) Atoji, M. *J. Chem. Phys.* **1967**, *47*, 1188.
- (25) Bader, R. W. F. *Chem. Rev.* **1991**, *91*, 893.
- (26) Cremer, D.; Kraka, E. *Angew. Chem., Int. Ed. Engl.* **1984**, *23*, 627.